J. Earth Syst. Sci. (2020)129 17
https://doi.org/10.1007/s12040-019-1293-4

Forming topography in granulite terrains: Evaluating the role of chemical weathering

Asmita Maitra[1], Aditi Chatterjee[1], Tirumalesh Keesari[2] and Saibal Gupta[1,*]

[1]*Department of Geology and Geophysics, Indian Institute of Technology Kharagpur, Kharagpur 721 302, India.*
[2]*Isotope and Radiation Application Division, Bhaba Atomic Research Centre (BARC), Mumbai 400 085, India.*
**Corresponding author. e-mail: saibl2008@gmail.com*

MS received 28 May 2019; revised 20 August 2019; accepted 30 August 2019

Granulite terrains have gently undulating topography, with charnockites and khondalites forming hillocks within low-lying areas comprising quartzofeldspathic gneisses (QFG). Petrographic, XRD and spectroscopic studies reveal that QFGs and charnockites show minimal clay mineral formation, indicating their resistance to chemical weathering. In contrast, khondalites weather progressively to form a variety of clay minerals, the proportion of which increases with elevation, ultimately stabilizing bauxite on hill-tops. Geochemical modelling indicates that this weathering pattern in khondalites can develop under open system conditions prevailing on hill tops and slopes, as rainwater is not retained within the system. This implies that the khondalite hills existed before bauxite formation. Since khondalite hills occur within more resistant but low-lying QFG, the present granulite terrain topography was not shaped by chemical weathering. Rather, mechanical weathering or neo-tectonic activity may be responsible for topography formation in stable granulite terrains.

Keywords. Granulite terrain; chemical weathering; monadnock; bauxitization; topography.

1. Introduction

In tectonically active regions on continents, prominent topographic features result from collisional orogenesis, volcanic arc formation and rifting; this first order 'young' topography is subsequently modified by weathering and erosion. Erosion rates in such areas of tectonically driven rock uplift are now believed to be controlled by increased rates of mechanical weathering processes such as landsliding (e.g., Montgomery and Brandon 2002). On the other hand, continental shield areas that are at present tectonically inactive typically preserve low elevation topography, tacitly assumed to result from long term degradation of earlier landscapes that have passed through an earlier stage of 'youth' (Holmes 1978). Such 'mature' or 'old' landscapes, characteristic of most shield areas, have faint relief with occasional isolated mounds or hills; these hills are commonly considered to represent residual topography or 'monadnocks' (Holmes 1978) or 'inselbergs' (Skinner and Porter 1995), defined by rock types that are resistant to weathering and erosion in comparison to associated lithologies. This is the topography commonly observed in granulite terrains in the Indian shield, such as the Eastern Ghats Belt (EGB), that are considered to represent sites of ancient collisional orogenesis (e.g., Gupta 2012; Dasgupta *et al.* 2013). Since these old, granulite terrains are not at present undergoing tectonically driven uplift, and the subdued

Published online: 20 December 2019

differential elevation is expected to limit mechanical weathering, chemical weathering may be considered to play a significant role in shaping their landscapes. Since this implies a switch in the relative importance of mechanical and chemical weathering processes as an orogen is eroded, an evaluation of the relative roles of mechanical or chemical weathering in creating granulite landscapes, that represent old orogens, can be of considerable interest.

In this study, we address this problem in an 'old' landscape within the EGB, a granulite terrane that borders the eastern fringe of the Bastar and Dharwar cratons in peninsular India (figure 1a). The northern part of the belt, where this study was carried out, is characterized by generally flat, low-lying topography interspersed with occasional jagged as well as rounded hillocks and mounds (figure 1d). We have conducted geological mapping across a representative part of this area, and through systematic petrographic, clay mineral and geochemical modelling studies, we suggest that even in such areas of modest topography, chemical weathering is unlikely to play a major role in creating relief. The implication is that mechanical weathering may be more important than chemical weathering even in shaping 'mature' and 'old' landscapes.

2. Geology of the study area

The Eastern Ghats Belt (EGB) mainly comprises granulite facies rocks, with migmatitic quartzofeldspathic gneiss (QFG), charnockite and khondalite as the main lithologies. These three major lithologies vary in proportion within distinct litho-tectonic units that are oriented parallel to the trend of the belt (Ramakrishnan *et al.* 1998). The northern part of the EGB is dominated by quartzofeldspathic gneisses and is referred to as the Charnockite Migmatite Zone (CMZ of Ramakrishnan *et al.* 1998; figure 1a). Further south, the Eastern and Western Khondalite Zones (EKZ and WKZ, respectively), and the Western Charnockite Zone (WCZ) generally show higher elevations, defining much of the 'Eastern Ghats' hill ranges in this region. Thus, the litho-tectonic units dominated by charnockites and khondalites (i.e., the WCZ, WKZ and EKZ) are elevated compared to the unit dominated by migmatitic quartzofeldspathic gneisses (i.e., the CMZ). Charnockites, khondalites and migmatitic quartzofeldspathic gneisses are all present within the CMZ. The presence of all these lithologies in close proximity in this unit of the EGB makes it easier to systematically study the differences in topographic elevation in relation to lithology, and to compare the weathering pattern in these different rock types both with respect to lithology and elevation.

3. Methodology

Since the CMZ contains all three major rock types of the EGB, a suitable area within this unit was selected for geological mapping. The selected area was almost completely accessible in all sectors, contains all three major lithologies, and has the characteristic undulating topography as indicated in GoogleEarth imagery as well as in the field (figure 1b, c). Comparison of the geological map prepared in this study (figure 1c) with the GoogleEarth image of the study area (figure 1b) allows evaluation of the correlation, if any, between lithology and elevation. The nature of weathering of khondalite, charnockite and quartzofeldspathic gneiss can be traced from the petrographic and spectroscopic analysis, and therefore, rock samples were collected from all rock types in the area, including weathered varieties. Khondalites showed a distinct difference in appearance and degree of weathering with elevation; thus, khondalite samples were collected both from topographically high (Sample no. 3B at an elevation of 255 m) and low regions (Sample no. 2 at 112 m and Sample no. 16A from 52 m) (figure 1c). Charnockite and quartzofeldspathic gneiss showed no such variation with elevation. For characterization, representative samples of the charnockite (Sample A11R) and QFG (Sample A18R) were selected for analysis (figure 1c). Petrographic studies of thin sections prepared from the rock samples were conducted using a LEICA DM 4500 P microscope, and the captured images were processed using the LeicaQwin software. To identify clay minerals that cannot be detected using the petrological microscope, FTIR analysis was conducted. For this, the rock samples were initially powdered and mixed with KBr powder, ground to a grain size less than 5 mm in diameter and pressed into a transparent pellet. This pellet was then analysed in a NICOLET 6700 model Fourier Transform Infra-Red (FTIR) spectrometer at the Central Research Facility (CRF), IIT Kharagpur, with a spectral resolution of 4 cm^{-1} in the Mid IR range

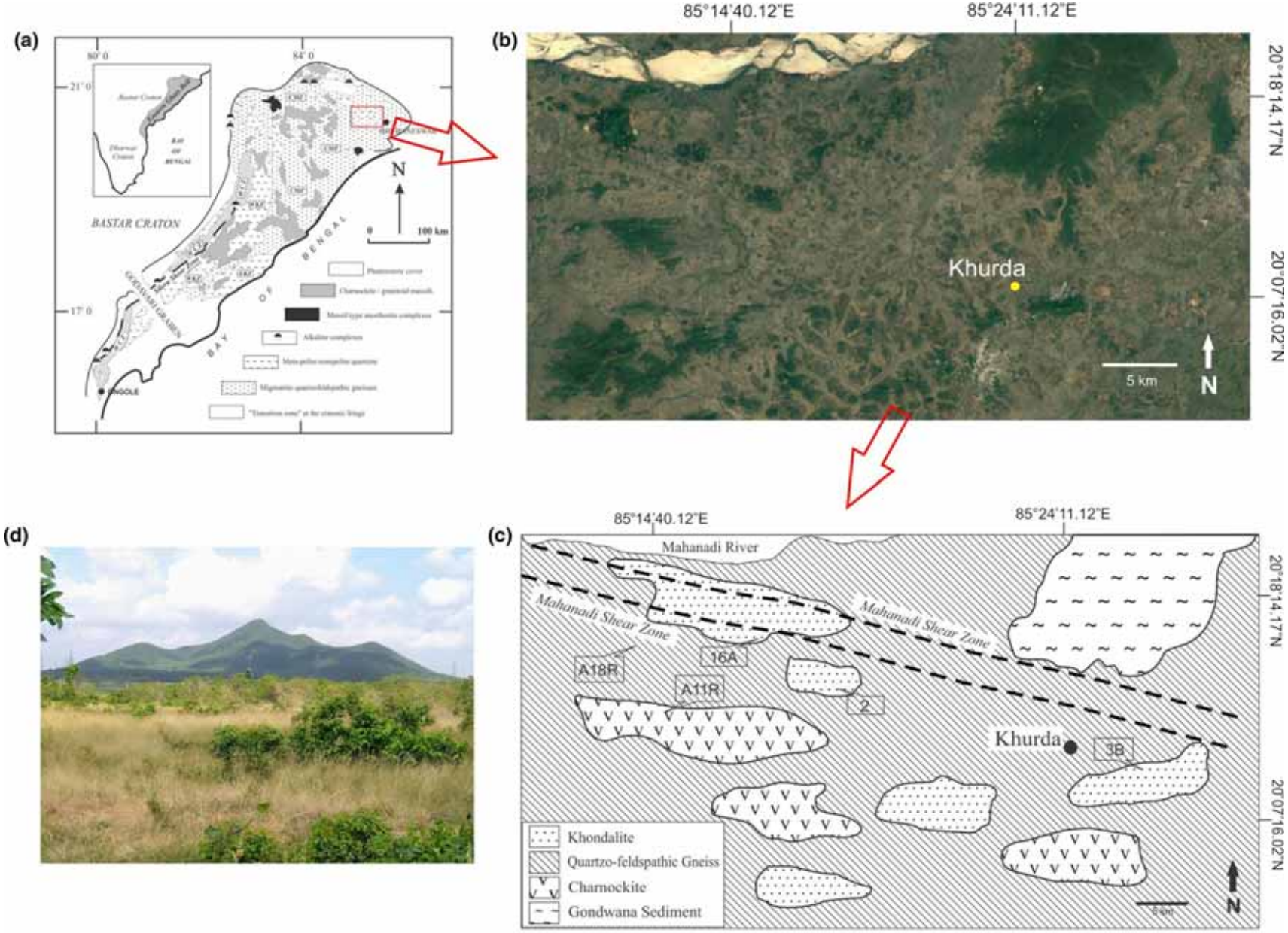

Figure 1. (**a**) Geological map of the Eastern Ghat Belt, redrawn after Ramakrishnan *et al.* (1998). Red box shows the exact position of the study area; **(b)** GoogleEarth Image of the study area; **(c)** Geological map of the area prepared in this study. **(d)** Isolated hills of khondalite overlying low-lying terrain of QFG.

(4000–400 cm^{-1}). For further confirmation of the major and clay mineral species, powder X-ray diffraction analyses of the whole samples were also conducted using a Bruker AXS D8 Diffractometer hosted in the Department of Chemistry, Indian Institute of Technology Kharagpur. Each sample was analyzed within the two-theta range 10°–90° using Cu–kα excitation with a 50 mA current and a power of 40 kV. Peaks obtained from XRD analyses were compared with the available online database using the X'pert HighScore Plus software. Finally, geochemical modelling of khondalite weathering was carried out using the geochemical modelling software, Geochemist's Workbench (GWB) v. 10.0.4 (Bethke 2007).

4. Results

4.1 *Geological mapping*

The study area mostly comprises migmatitic quartzofeldspathic gneiss (QFG), khondalite and charnockites (figure 1c). Sheet-like exposures of quartzofeldspathic gneiss form flat-lying areas of low topography between the elevated hills. These sheet outcrops often lie in the middle of paddy fields, and are generally so completely planed that it is difficult to measure foliation orientation in outcrop. Charnockites invariably form hillocks within the region, similar to the khondalites, but charnockite hillocks tend to be more rounded. Charnockite mounds are generally poorly vegetated, and exposure freshness remains similar at the bases and tops of the hills. Khondalites also form hillocks in the region, varying from jagged, cone-like features to less common low elevation rounded mounds. Interestingly, relatively fresh khondalites can be collected from small mounds, or the lower reaches of high khondalite hillocks; the degree of weathering of the khondalites increases with elevation, with the crests of the highest khondalite hills being the most weathered. At the top of some of these high hills khondalites are extremely weathered and vegetation is dense, indicating the presence of a well-developed soil cover that testifies to greater weathering of khondalites at higher elevations.

4.2 *Petrography*

Petrographic analysis of rock samples collected from the study area shows the effects of chemical weathering. The QFGs are characterized by leucocratic and melanocratic segregation layering. Biotite-poor leucocratic layers consist of quartz and plagioclase feldspar, whereas the melanocratic layers are predominantly composed of biotite and garnet. Plagioclase and alkali feldspar grains are deformed and recrystallized. All phases, including feldspars, have perfectly preserved grain boundaries and are mostly unaltered (figure 2a). Charnockites show weathering patterns similar to the QFGs. Fresh grains of quartz, plagioclase feldspar, biotite, garnet and orthopyroxene are seen in thin section (figure 2c). Two foliation generations are observed, an earlier high grade foliation defined by orthopyroxene cut across by a later, retrogressive foliation defined by biotite which partially to completely replaces orthopyroxene in many places. Khondalites in the area show a distinct variation in the degree of weathering, and are classified into three groups: slightly weathered khondalite, weathered khondalite and extremely weathered khondalite. The mineralogy within the segregation layering of these rocks is always clearly identifiable irrespective of the degree of weathering. In the slightly weathered khondalite, layers composed of quartz and alkali feldspar alternate with layers of garnet and sillimanite (figure 2e). Garnets are fresh with inclusions of quartz and have prominent grain boundaries. Elongated sillimanite needles have a preferred orientation parallel to the lineation direction. Minerals within the weathered khondalite (figure 2g) are more fractured than in the slightly weathered variety, with the formation of clay minerals within the fractures that could not be identified under the microscope. Garnet and feldspar grains show alteration, with much of the feldspar alteration occurring along the cleavage traces. The segregation banding is still distinct. Unlike the slightly weathered variety, the weathered khondalites also show a significant increase in the proportion of opaque minerals. Extremely weathered khondalites (figure 2i) show a high proportion of clay minerals (individual phases not distinguishable under the microscope), followed by quartz, sillimanite, garnet and alkali feldspar, in decreasing order of abundance. In these rocks highly altered garnet grains occur as brown patches; no prominent grain boundaries can be observed. A close-spaced segregation layering is present with quartz and altered alkali feldspar defining thicker layers, while and the weathered relict garnet grains and altered clay minerals define thinner layers. Very small amounts of altered biotite and sillimanite survive in some samples.

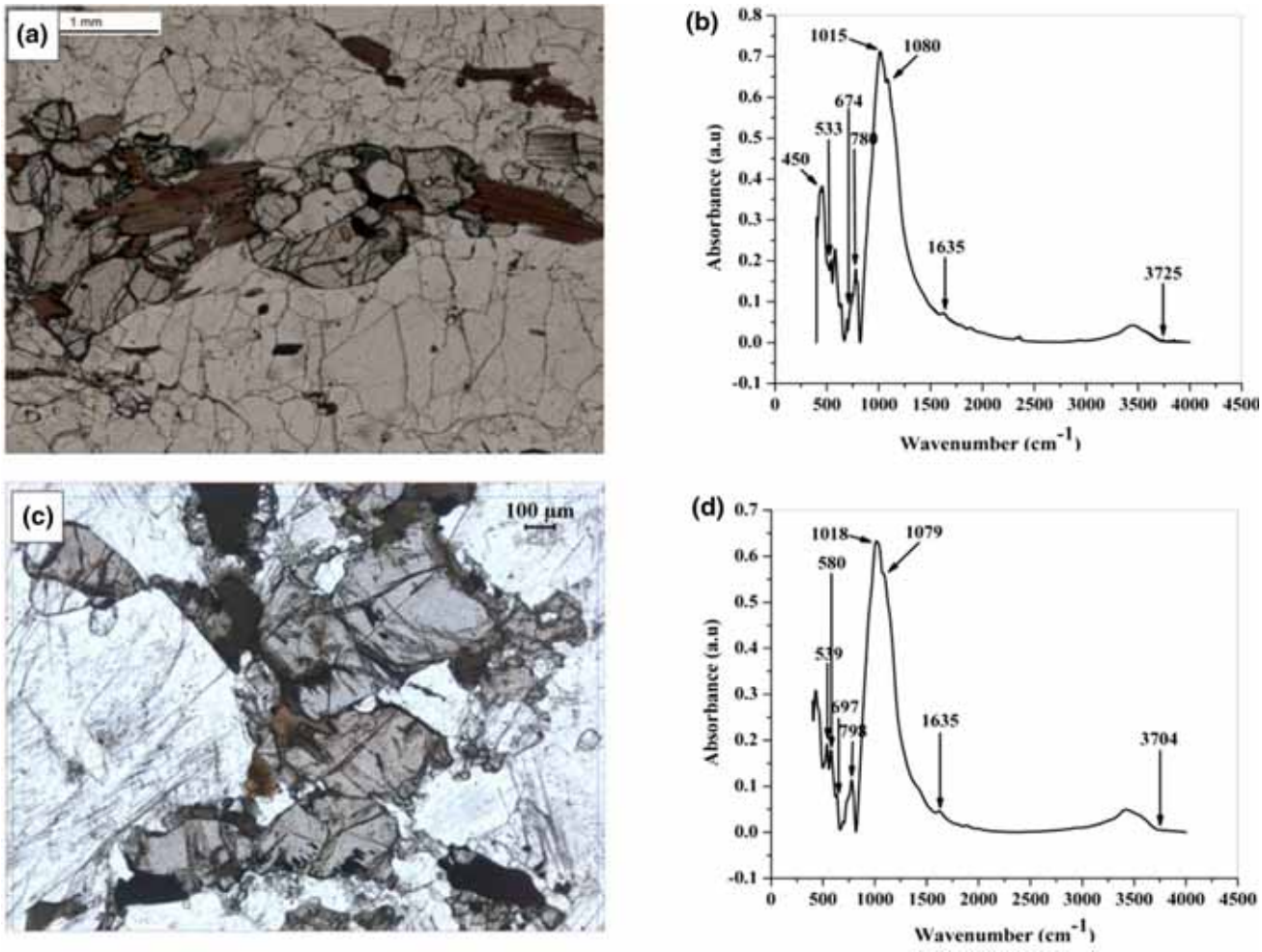

Figure 2. Photomicrographs of rock types with corresponding FTIR spectra from the study area. (**a** and **b**) Quartzofeldspathic gneiss; (**c** and **d**) Charnockite; (**e** and **f**) slightly weathered khondalite; (**g** and **h**) weathered khondalite; and (**i** and **j**) extremely weathered khondalite (for further information see the text).

4.3 *Spectroscopic analysis*

FTIR analysis was conducted on samples of quartzofeldspathic gneiss, charnockite and the three different categories of khondalite, and the spectra obtained have been compared with those from previous studies (Farmer 1974; Frost *et al.* 1999). Absorbance spectra for the QFG samples are shown in figure 2(b), where absorbance peaks occur at different wavenumbers indicating the presence of different minerals. Peaks at 1080 cm^{-1} for Si–O stretching vibration, 780 cm^{-1} for Si–O symmetric stretching and at 450 cm^{-1} for asymmetric Si–O bending represent the presence of quartz; OH stretching at 3725 cm^{-1} indicates the presence of micas, most probably biotite, while the absorptions at 1015, 674 and 533 cm^{-1} define the presence of feldspar. A lower intensity peak at 1635 cm^{-1} indicates the presence of a small amount of montmorillonite, the diagnostic peak for this mineral. Figure 2(d) shows the absorption pattern obtained from the analyzed charnockite sample. T–O stretching vibration peaks at 1079 and 539 cm^{-1} confirm the presence of pyroxene. An absorbance peak at 3704 cm^{-1} occurs due to the OH stretching vibration of biotite, consistent with the presence of this mineral in charnockite. Presence of feldspar, quartz and garnet in the charnockite are confirmed from the Si(Al)–O stretching peak at 1018 cm^{-1}, Si–O stretching at 798 and 697 cm^{-1}, and the SiO_4 vibration peak at 580 cm^{-1}, respectively. The charnockite sample also shows a 1635 cm^{-1} peak confirming the presence of a small amount of montmorillonite. The absorbance versus wave number plots for the khondalite samples show gradual changes in amount and species of the clay minerals with increasing weathering. Figure 2(f) shows the characteristic spectra obtained from the slightly weathered khondalite sample. The absorbance

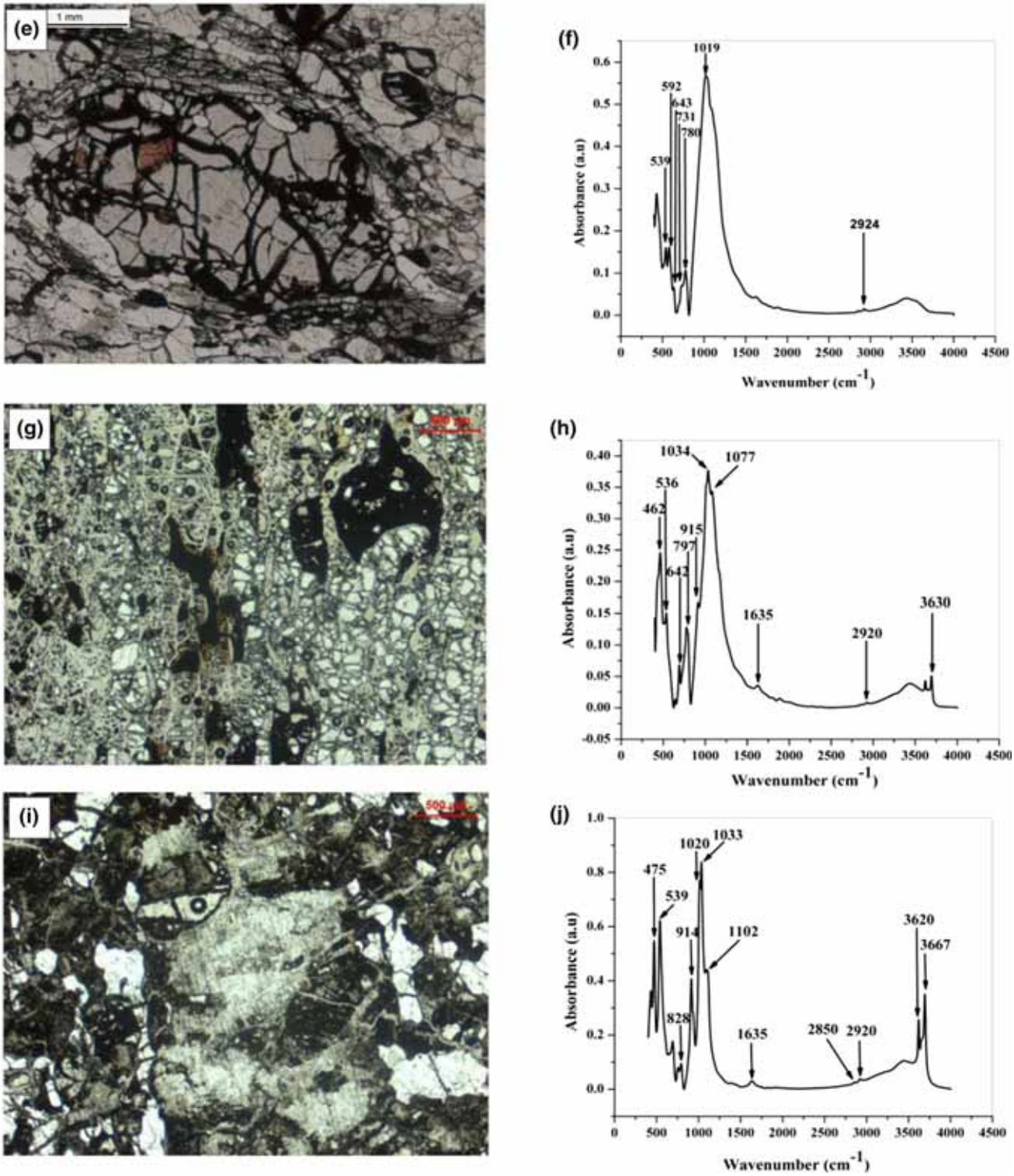

Figure 2. *(Continued.)*

peaks at 539 and 643 cm^{-1} are associated with the SiO_4 vibration and tetrahedral Fe^{3+} in garnet, respectively. The 592 cm^{-1} peak occurs due to O–Si(Al)–O bending in feldspar. The absorbance band at 731 cm^{-1} is due to Al–O stretching, and vibration of oxygen in the Al–O–Si bond of sillimanite. The 1019, 780 and 2924 cm^{-1} peaks occur due to the Si–O stretching for kaolinite, Si–O symmetric stretching for quartz and OH stretching for diaspore, respectively. The analysed spectrum for the weathered khondalite sample is given in figure 2(h). Absorbance peaks at different

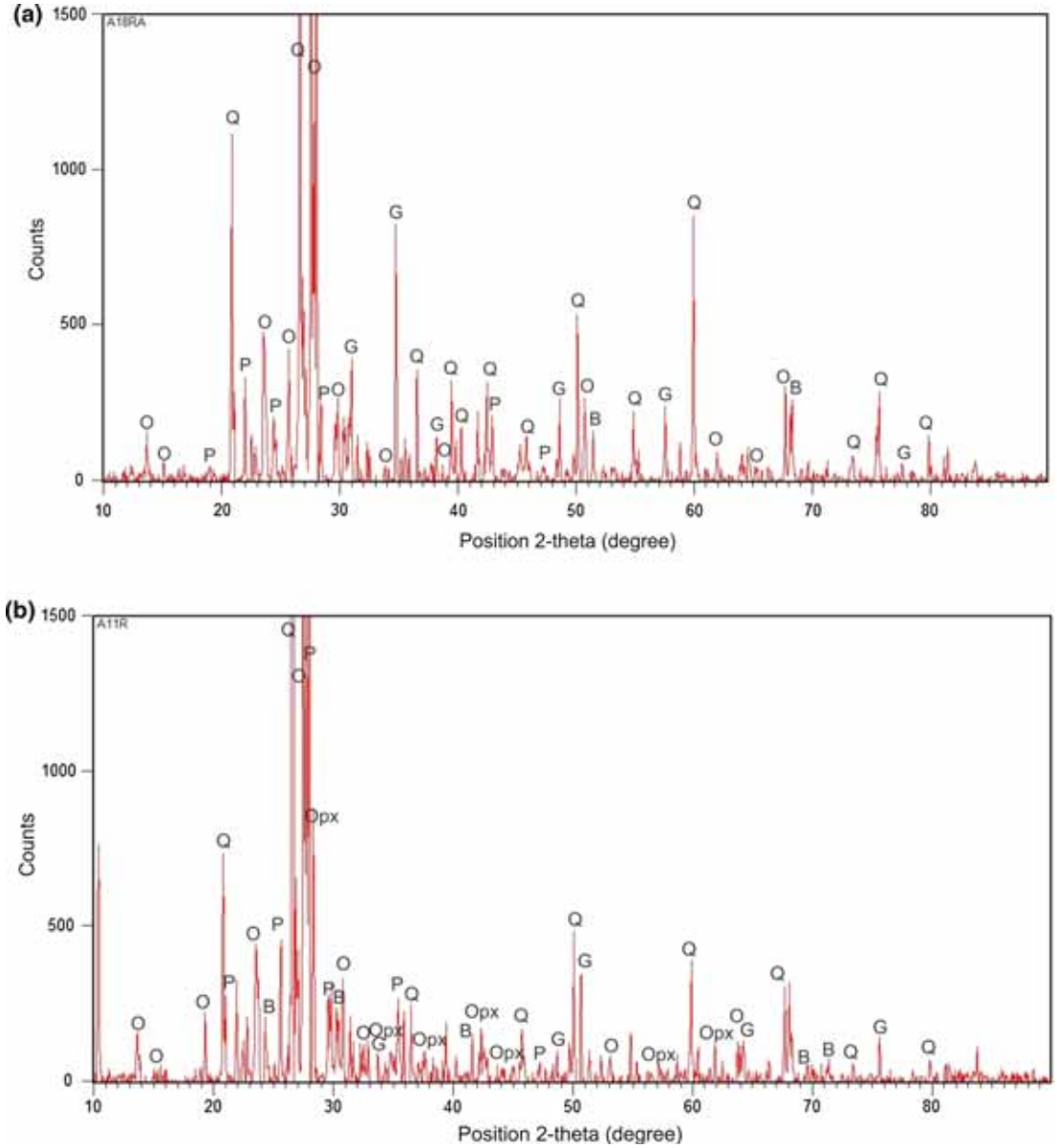

Figure 3. XRD spectra of a representative **(a)** QFG (A18R) and **(b)** charnockite (A11R) sample. Major minerals are identified from the respective peaks. Abbreviations. Q: Quartz, O: Orthoclase feldspar, P: Plagioclase feldspar, B: Biotite, G: Garnet and Opx: Orthopyroxene.

wavenumbers define the presence of illite, montmorillonite, goethite, diaspore, kaolinite, garnet and quartz. Peaks at 462 and 642 cm^{-1} occur due to Si–O stretching vibration in quartz and SiO_4 vibration in garnet, respectively. Peaks representing kaolinite are present at 536 cm^{-1}, which occur due to Fe–O, Fe_2O_3 and Si–O–Al stretching, and at 1034 cm^{-1}, representing Si–O stretching. Absorbance peaks at 3630, 915, 1635, 2920 and 1077 cm^{-1} occur due to the OH stretching vibration in the octahedral sites in illite, Al–OH–Al bending vibration in illite, OH bending vibration in montmorillonite, OH stretching vibration in goethite and OH bending vibration in diaspore, respectively. Importantly, spectral signatures of feldspar and sillimanite cannot be detected, although minor amounts are identifiable petrographically. Figure 2(j) shows the absorbance spectra of the extremely weathered khondalite sample. Most of the mineralogy is dominated by clay minerals, i.e., gibbsite, diaspore, goethite, illite, montmorillonite and kaolinite. Intense absorption bands at 3620, 3667, 2920 and 2852 cm^{-1} are due to OH stretching vibration of gibbsite, diaspore and goethite, respectively. Gibbsite is also defined by the absorption peaks at 914 and 1020 cm^{-1} due to the OH bending vibration, and 1102 cm^{-1} due to Al–OH bending.

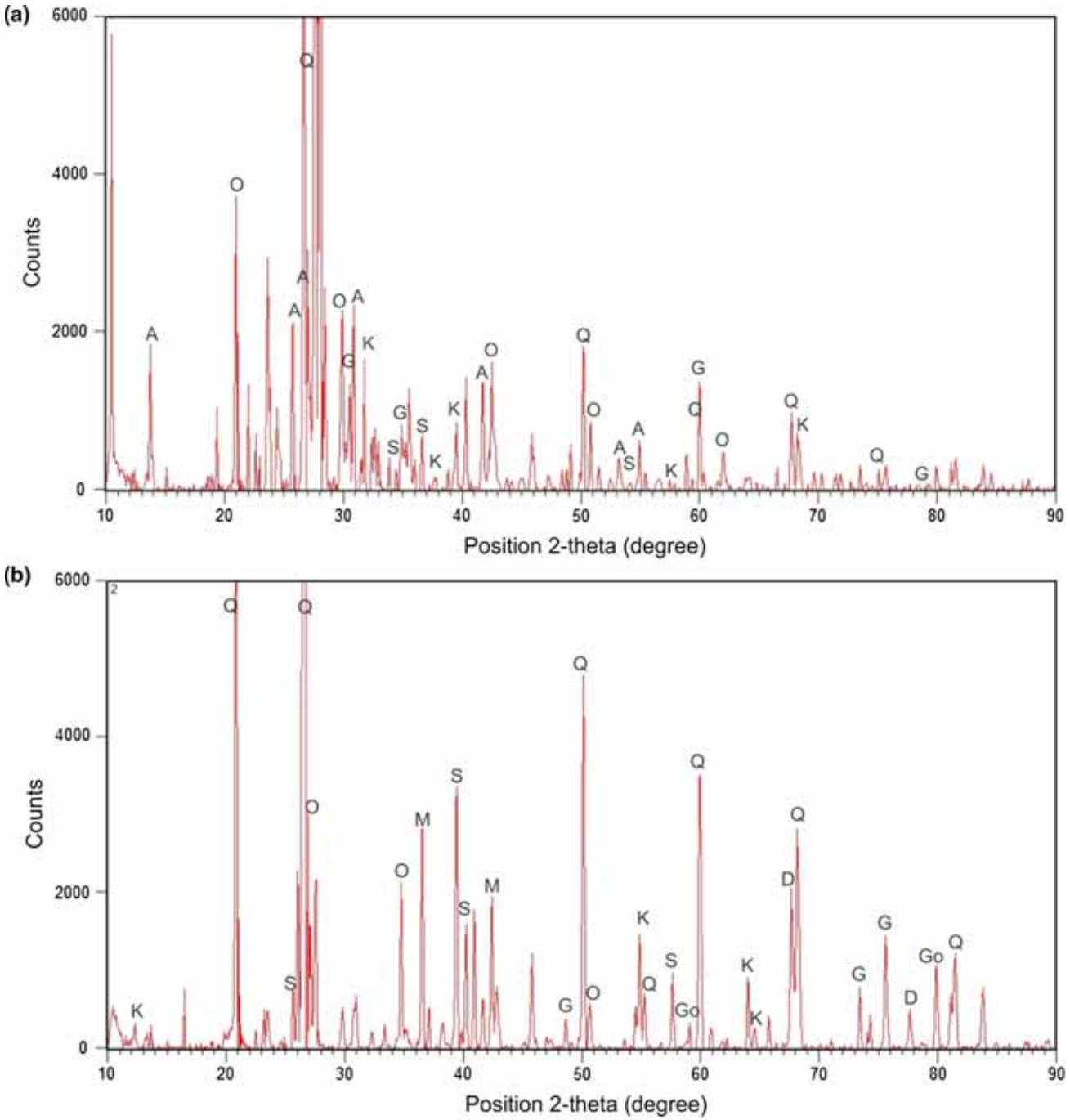

Figure 4. XRD spectra of **(a)** slightly weathered khondalite (Sample 16A), **(b)** weathered khondalite (Sample 2) and **(c)** extremely weathered khondalite (Sample 3B). Both major and clay minerals are identified from their respective peaks. Abbreviations. Q: Quartz, O: Orthoclase feldspar, P: Plagioclase feldspar, B: Biotite, G: Garnet, K: Kaolinite, S: Sillimanite, M: Montmorillonite, D: Diaspore, Go: Goethite, C: Cordierite and Gi: Gibbsite.

Although some of the characteristic peaks of goethite and gibbsite overlap with each other, the OH bending vibrations at 1020 and 928 cm^{-1} are diagnostic of goethite. The peaks at 475, 539 and 1033 cm^{-1} are the clearest proof for the presence of kaolinite occurring due to Si–O–Si bending, Fe–O, Fe_2O_3, Si–O–Al stretching and Si–O stretching, respectively. Presence of illite and montmorillonite are defined by the absorbance at 828 cm^{-1} due to Al–OH–Mg vibration, and 1635 cm^{-1} due to OH bending vibration, respectively. For this extremely weathered khondalite sample, the presence of gibbsite, a bauxite component, is very important; this is not present in any other rock type.

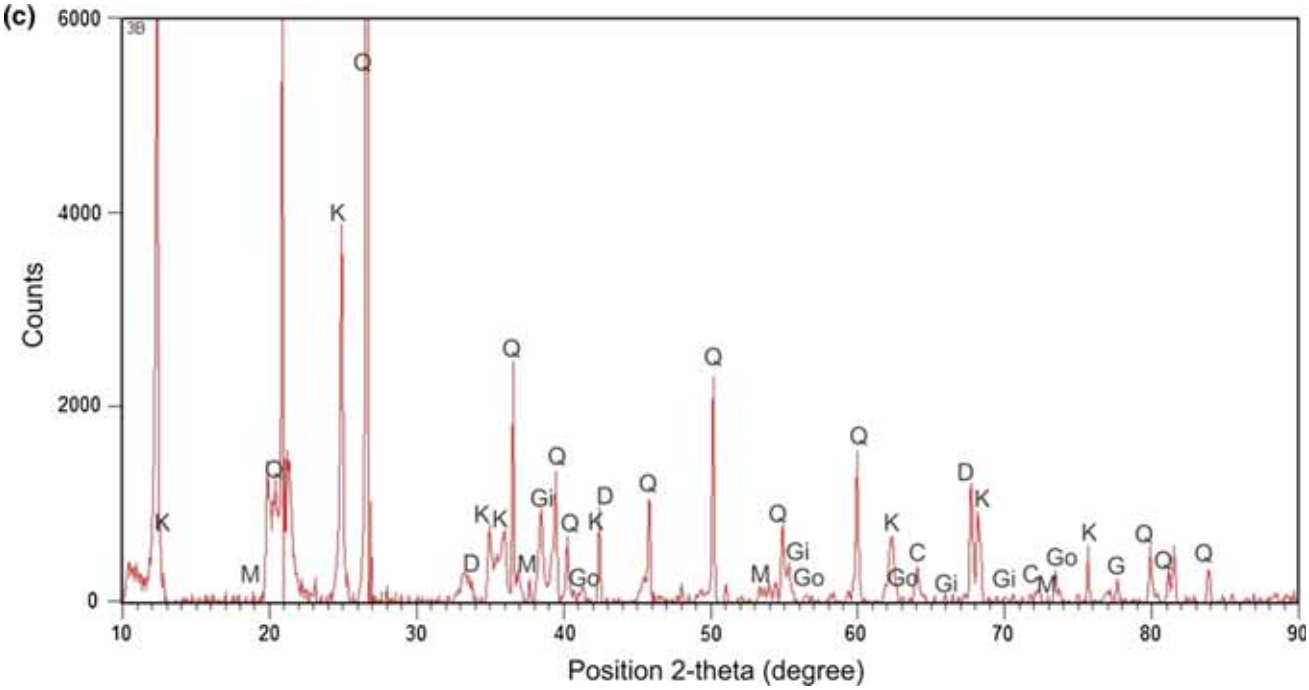

Figure 4. *(Continued.)*

Table 1. *Average chemical composition of rain water (after Das et al. 1994) used in the geochemical modelling calculations.*

Constituents	Concentration (mg/l)
Na^+	2.31
K^+	0.57
Mg^{2+}	0.42
Ca^{2+}	3.62
Cl^-	4.87
SO_4^-	1.04
NO_3^-	1.08
pH	6.89

Table 2. *Mineral modal proportions in khondalite used for geochemical modelling.*

Minerals	Wt%
Quartz	35.24
Garnet	29.09
Sillimanite	19.36
Orthoclase	12.26
Plagioclase	1.76
Biotite	2.13

4.4 *X-ray diffraction analysis*

Figure 3 shows the major X-ray peaks obtained from the QFG and charnockite samples. In the QFG sample (figure 3a), major peaks of quartz can be identified at 20.85°, 26.66°, 36.52°, 40.29°, 42.44°, 50.14°, 59.91°, 75.64° and 73.42°. Apart from quartz, major peaks corresponding to garnet occur at 34.74°, 38.21°, 48.63° and 57.52°, and for plagioclase feldspar at 18.98°, 22°, 24.36°, 28.04°, 42.93° and 47.25°. Orthoclase feldspar is characterized by the peaks at 13.66°, 15.09°, 23.57°, 25.67°, 29.83°, 34.75°, 38.72°, 61.93° and 65.25°. No clay mineral was detected by the XRD analysis of the QFG sample. X-ray peaks obtained from the charnockite (figure 3b) indicate the presence of quartz, plagioclase feldspar, orthoclase feldspar, orthopyroxene, garnet and biotite. Peaks at 26.56°, 36.49°, 45.74°, 50.08°, 59.83°, 67.62°, 73.39° and 79.26° define quartz; the peaks at 21.95°, 27.99°, 30.32°, 35.89° and 47.20° indicate plagioclase feldspar; peaks at 13.64°, 15.08°, 19.27°, 23.55°, 27.50°, 30.80°, 32.24°, 47.21°, 64.23° and 73.40° define orthoclase feldspar; peaks at 34.75°, 35.42°, 52.28°, 45.80°, 57.15° and 61.86° signify orthopyroxene, whereas garnet is indicated by the characteristic peaks at 34.75°, 48.63°, 55.40° and 75.59°. The presence of biotite is confirmed by the 24.32°, 20.81°, 41.62° and 69.57° peaks. In the khondalite samples, apart from the major minerals, clay minerals are also identified from the characteristic X-ray peaks. Figure 4 shows the major peaks of the respective minerals that constitute the three different categories of khondalites. Slightly weathered khondalite (figure 4a) contains quartz, albite, orthoclase feldspar, sillimanite, garnet and

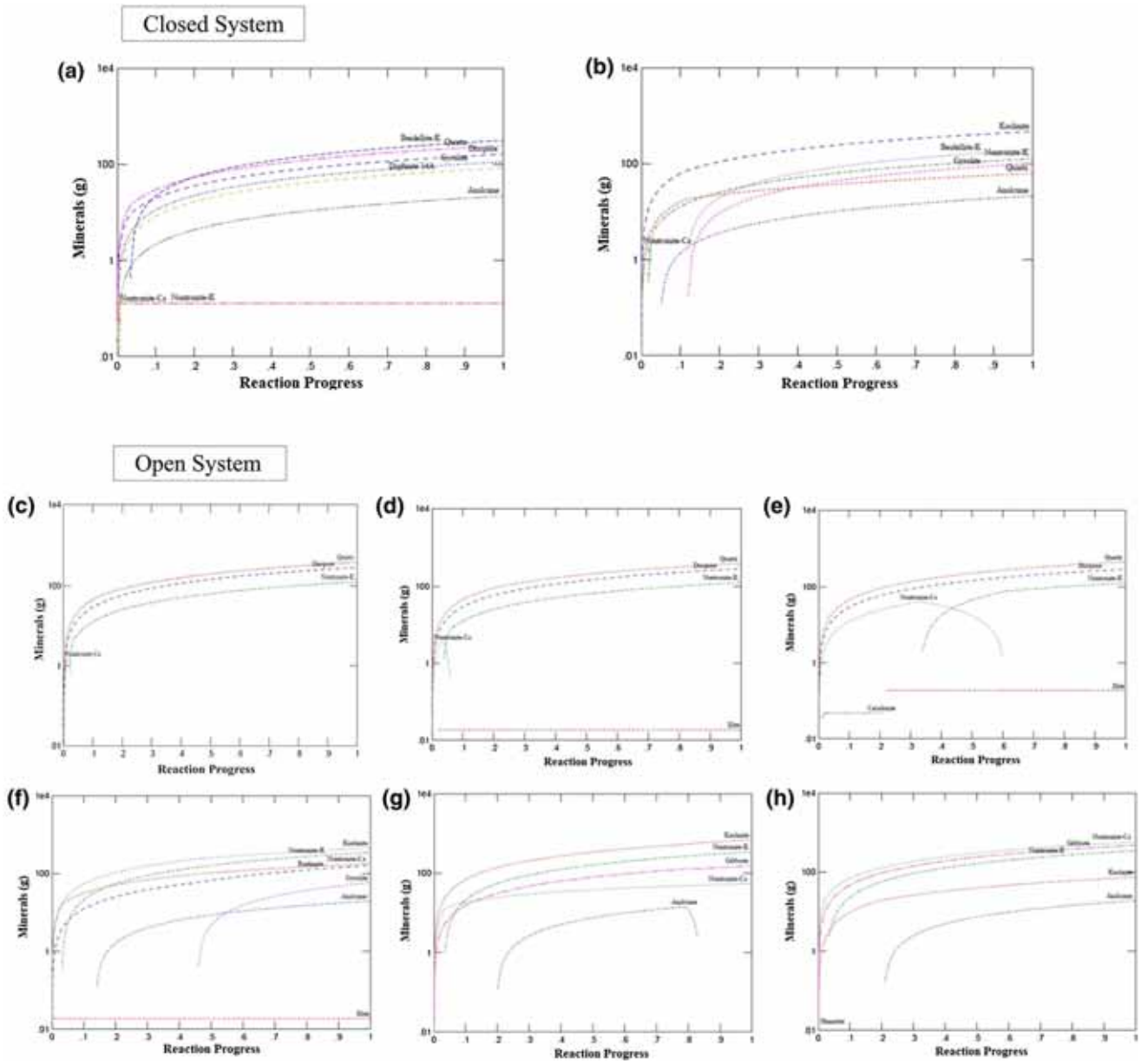

Figure 5. Results of geochemical modelling of weathering in khondalite. The figures show the sequence of minerals produced with reaction progress under (a–b) closed system; and (c–h) open system conditions. Note that gibbsite only stabilizes in the final stages of weathering under open system conditions.

kaolinite as major constituents. Characteristic peaks of kaolinite occur at 32.48°, 37.76°, 39.46°, 57.92° and 68.28°. In the weathered khondalite sample (figure 4b), XRD analysis confirms the presence of montmorillonite, goethite, kaolinite and diaspore. Occurrence of gibbsite, diaspore, montmorillonite and goethite in the extremely weathered khondalite sample (figure 4c) is confirmed from the diagnostic peaks in the X-ray spectrum. Peaks at 37.74°, 55.34°, 65.94° and 70.55° are consistent with the presence of gibbsite in this sample.

4.5 *Modelling of chemical weathering in khondalite*

As demonstrated in section 4.3, khondalites show the most substantial change in clay mineral species with increasing intensity of weathering, and it was therefore decided to simulate the weathering of this rock type using the geochemical modelling software GWB (Bethke 2007). Water–rock interaction in khondalite is modelled in both closed and open systems at a temperature of 25°C. The initial water composition was assumed to be the same as that of

rainwater (Das *et al.* 1994; table 1). The rock composition used in the calculations is given in table 2. The gas composition was assumed to be atmospheric. In the water–rock interaction models, 1 kg of rock was initially reacted with 0.5 kg of water. With time, the water:rock ratio increases as porosity increases with increasing weathering. Since this water–rock interaction modelling is solely based on thermodynamic calculations, formation of a few clay minerals was suppressed as they are not kinetically favoured; also, no evidence of these minerals was detected during FTIR spectroscopy. At first, modelling was done for a closed system (figure 5), in which both the water and rock compositions consistently adjust to ongoing reaction. Under these closed system conditions, chemical reactions between minerals in the rock and water take place within the pore spaces of the rock itself, and a large number of different minerals are produced as reaction progresses. Beidellite, quartz, diaspore, gyrolite, daphnite and analcime show an increasing trend a reaction continues, while nontronite-Ca and nontronite-K maintain constant proportions throughout the reaction duration. Kaolinite forms with further progress of reaction and has the highest proportion among different products in the final stages.

Subsequently, modelling was done for an open system (figure 5) where the composition of rock and water was constantly allowed to change. At the initial stage, fresh khondalite in the presence of water reacts to form diaspore, nontronite-K and nontronite-Ca. As reaction proceeds further due to increase in porosity, the water:rock ratio increases, leading to the formation of illite along with quartz, nontronite-K and nontronite-Ca. Nontronite-Ca disappears with further reaction progress, while the amount of nontronite-K increases, and a new mineral (celadonite) forms which then gives away to illite. Boehmite, gyrolite, analcime and kaolinite form as reaction products with further reaction progress. At the next stage, gibbsite is produced as a reaction product; this is a major component of bauxite and an alteration product of many aluminous and aluminosilicate minerals under intense weathering conditions. With further reaction, the concentration of all the weathering products increases; importantly, gibbsite is produced in larger amount than kaolinite. Thus, gibbsite is only produced as the final weathering product of khondalite under open system conditions; under closed system conditions, no gibbsite is formed, and kaolinite represents the most extreme product of chemical weathering.

5. Discussion and conclusions

Correlation of the geological map prepared in this study (figure 1c) with the GoogleEarth image (figure 1b) clearly shows that most of the elevated hillocks in the area are composed of charnockite (maximum elevation 280 m) or khondalite (maximum elevation 254 m), while the flat, low-lying intervening area comprises migmatitic quartzofeldspathic gneiss (maximum elevation 47 m). Petrographic study and XRD analyses of samples from all these rock types indicate that the charnockites and QFG preserve their original, unweathered mineralogy, with only minimal alteration. On the other hand, the khondalite samples show a wide range in the extent of weathering, varying from samples with well-preserved metamorphic mineral assemblages (slightly weathered khondalite), through more extensively weathered varieties (weathered khondalite), to extremely weathered khondalites that retain very little of the original mineralogy. While the XRD analyses do not show any signatures of clay mineral development in the QFG and charnockite, FTIR spectroscopy of these samples do show minor clay mineral development, with spectral signatures of primary minerals largely retained; this suggests that both these rock types have only undergone minimal chemical weathering, consistent with field and petrographic observations. On the other hand, clay mineral development is profuse in the khondalites, varying from kaolinite in the slightly weathered varieties, through illite, montmorillonite, goethite, diaspore and kaolinite in weathered samples, finally, to an assemblage of all the above minerals, along with gibbsite, in the extremely weathered khondalite. Figure 2 shows that the IR spectra of khondalites change with increasing weathering intensity, with an increase in the proportion of clay minerals. Gibbsite and goethite are not observed in spectra from the slightly weathered khondalite sample. The extremely weathered khondalite sample, on the other hand, contains diaspore and gibbsite, and therefore defines the initiation of bauxitization. Importantly, these extensively weathered khondalites are almost exclusively restricted to the tops of the high hillocks in the area, while khondalite exposures at lower elevations are distinctly less weathered. Thus, from the petrography, XRD and FTIR studies, it can be demonstrated that elevation has an important role to play in the weathering of the khondalite hills.

The documented variation in the intensity of weathering of the khondalites with elevation is explained by the results of geochemical modelling. Under closed system conditions, khondalites do not stabilize gibbsite in the clay mineral assemblage, but do so extensively under open system conditions. As argued by Mitra *et al.* (2016), open system conditions simulate the existence of slopes (or topography) in nature; elevated regions with slopes ensure that precipitating rain water is continuously removed from the system after interacting with the rock mass, along with its soluble components. This is consistent with the stabilization of gibbsite by weathering of khondalite at higher elevations; at lower heights, where slopes are subdued, the system is more likely to retain stagnant water, thereby inhibiting gibbsite formation. This model also explains why bauxites form from khondalites at hill tops. Interestingly, the celebrated "East Coast Bauxite" deposits of the EGB are located on top of khondalite hills within the WKZ and EKZ. This region, characterized by bauxite capping upon flat-topped khondalite hills, stretches over a distance of 200–250 km in the EGB (Deb and Joshi 1984; Devaraju and Khanadali 1993; Bhukte and Chaddha 2014).

This study therefore shows that although both charnockites and khondalites form hillocks within a low-lying migmatitic QFG terrain, they show markedly variable response to chemical weathering. Khondalites clearly respond more actively to chemical weathering processes, unlike charnockites and QFGs, and there is little reason for khondalites to form monadnocks if erosion in these terrains was dominantly controlled by such processes. On the other hand, charnockites and QFGs are both resistant to chemically driven erosion processes, and therefore, their differential elevation cannot be explained by chemical weathering. It can therefore be concluded that the undulating topography of the EGB, and possibly other granulite terrains is not controlled by chemical weathering processes.

This conclusion raises an intriguing question – what then is responsible for the creation of topography in these terrains? There are two possible alternatives – the first is that the differential weathering is controlled by mechanical, rather than chemical weathering. However, mechanical weathering is generally most effective in terrains where differential elevation already exists, as in modern orogenic belts; thus, enhanced rates of mechanical weathering are more likely to be the *result*, rather than the *cause*, of topography formation in mature terrains. The other alternative has more exciting implications – that the topography even in these mature terrains is actually a manifestation of present-day crustal stresses and possibly reflects slow but active neo-tectonic activity. It is being increasingly realized that continental interiors are zones of slow strain accumulation, and may therefore be vulnerable to seismic and associated natural hazards (e.g. Landgraf *et al.* 2016). Indeed, microseismic activity has been documented in the EGB, close to the present study area (Gupta *et al.* 2014), and therefore, the second possibility cannot be completely overruled. It is of interest to determine the extent to which slow active tectonic processes result in topography formation in continental interiors, although this falls beyond the scope of this study. Nevertheless, what may be inferred is that the topography of old and mature terrains may potentially reveal more about crustal stress conditions than is currently realized.

Acknowledgements

The main funding for this study was from the RTAC-BRNS project scheme, India (Sanction No. 35/14/12/2016-BRNS/35049) to SG. AM thanks IIT Kharagpur and the Ministry of Human Resource Development (MHRD), Department of Higher Education, New Delhi, India for providing the regular student assistantship. AM conveys her sincere gratitude to the Department of Geology and Geophysics, IIT Kharagpur for facilitating this study, and Prof. Kumar Biradha of the Department of Chemistry, IIT Kharagpur, for facilitating the XRD analysis. Additional support and discussion with Kaushik Mitra and Himela Moitra, Department of Geology & Geophysics, IIT Kharagpur, were also extremely useful. The paper has benefited greatly from the comments of the handling editor and two anonymous referees.

References

Bethke C M 2007 *Geochemical and Biogeochemical Reaction Modeling*; Cambridge University Press, New York.

Bhukte P and Chaddha M 2014 Geotechnical evaluation of eastern Ghats bauxite deposits of India; *J. Geol. Soc. India* **84** 227–238.

Das S, Mehta B C, Singh R V and Srivastava S K 1994 Chemical Composition of rainwater over Bhubaneshwar,

Orissa India; *Mausam, Ind. J. Met. Hydro.l Geophys. (Q)* **45** 255–260.

Dasgupta S, Bose S, and Das K 2013 Tectonic evolution of the Eastern Ghats belt, India; *Precamb. Res.* **227** 247–258.

Deb M and Joshi A 1984 Petrological studies on two East Coast bauxite deposits of India, and implications on their genesis; *Sedim. Geol.* **39** 121–139.

Devaraju T and Khanadali S 1993 Lateritic bauxite profiles of South-western and southern India characteristics and tectonic significance; *Curr. Sci.* **64** 919–921.

Farmer V C 1974 *The infrared spectra of minerals* (ed.) V C Farmer, London Mineralogical Society, 539p.

Frost R L, Kloprogge J T, Russell S C and Szetu J L 1999 Vibrational Spectroscopy and Dehydroxylation of Aluminum (Oxo)hydroxides: Gibbsite; *Appl. Spectrosc.* **43(4)** 423–434.

Gupta S (2012) Strain localization, granulite formation and geodynamic setting of 'hot orogens': A case study from the Eastern Ghats Province, India; *Geol. J.* **47(23)** 334–351.

Gupta S, Mohanty W K, Manda A and Misra S 2014 Ancient terrane boundaries as probable seismic hazards: A case studyfrom the northern boundary of the Eastern Ghats Belt, India; *Geosci. Frontiers* **5** 17–24.

Holmes A 1978 *Principles of Physical Geology; revised by Doris Holmes* (3rd edn), Wiley, New York, 730p.

Landgraf A, Kuebler S, Hintersberger E and Stein S 2016 Active tectonics, earthquakes and palaeoseismicity in slowly deforming continents; In: *Seismicity, Fault Rupture and Earthquake Hazards in Slowly Deforming Regions* (eds) Landgraf A, Kuebler S, Hintersberger E and Stein S, *Geol. Soc. London, Spec. Publ.* **432,** http://doi.org/10.1144/SP432.13.

Mitra S, Mitra K, Gupta S, Bhattacharya S, Chauhan P and Jain N 2016 Alteration and submergence of basalts in Kachchh, Gujrat, India: Implications for the role of the Deccan Traps in the India–Seychelles break-up; *Geol. Soc. London Spec. Publ.* **445** 171–196.

Montgomery D R and Brandon M T 2002 Topographic controls on erosion rates in tectonically active mountain ranges; *Earth Planet. Sci. Lett.* **201** 481–489.

Ramakrishnan M, Nanda J K and Augustine P F 1998 Geological evolution of the Proterozoic Eastern Ghat Mobile Belt; *Geol. Surv. India Spec. Publ.* **44** 1–21.

Skinner B J and Porter S C 1995 T*he Dynamic Earth: An introduction to Physical Geology* (3rd edn) John Wiley & Sons, Inc., 567p.

Corresponding editor: N V Chalapathi Rao